mathematics

Article

A NumericalInvestigation for a Class of Transient-State Variable Coefficient DCR Equations

Mohammad Ivan Azis

Department of Mathematics, Hasanuddin University, Makassar 90245, Indonesia; ivan@unhas.ac.id

Abstract: In this paper, a combined Laplace transform (LT) and boundary element method (BEM) is used to find numerical solutions to problems of anisotropic functionally graded media that are governed by the transient diffusion–convection–reaction equation. First, the variable coefficient governing equation is reduced to a constant coefficient equation. Then, the Laplace-transformed constant coefficients equation is transformed into a boundary-only integral equation. Using a BEM, the numerical solutions in the frame of the Laplace transform may then be obtained from this integral equation. Then, the solutions are inversely transformed numerically back to the original time variable using the Stehfest formula. The numerical solutions are verified by showing their accuracy and steady state. For symmetric problems, the symmetry of solutions is also justified. Moreover, the effects of the anisotropy and inhomogeneity of the material on the solutions are also shown, to suggest that it is important to take the anisotropy and inhomogeneity into account when performing experimental studies.

Keywords: transient; diffusion convection reaction; anisotropic; functionally graded materials; simulation

MSC: 35N10; 65N38

check for updates

Citation: Azis, M.I. A Numerical Investigation for a Class of Transient-State Variable Coefficient DCR Equations. *Mathematics* **2023**, *11*, 2091. https://doi.org/10.3390/math11092091

Academic Editors: Cuiying Jian and Aleksander Czekanski

Received: 11 April 2023
Revised: 25 April 2023
Accepted: 26 April 2023
Published: 28 April 2023

1. Introduction

Insights on flow in porous media may be obtained from [1–4]. Over the last ten years, functionally graded materials (FGMs) have become a popular research topic, and many studies have been conducted on FGMs for various applications. FGMs are defined by authors as materials that are inhomogeneous and have properties such as thermal conductivity, hardness, toughness, ductility, and corrosion resistance, which change spatially in a continuous manner. Commonly, the properties of the considered material for a specific application are represented by the coefficients of the governing equation. In this case, the coefficients should be constant if—and only if—the material is homogeneous.

The diffusion convection reaction (DCR) equation is usually used as the governing equation for many applications in engineering, medicine, biology, and ecology. Several studies have been conducted to find numerical solutions to the DCR equation. These studies include Fendoğlu et al. [5] in 2018, Wang and Ang [6] in 2018, Sheu et al. [7] in 2000, Xu [8] in 2018, and AL-Bayati and Wrobel [9] in 2019, who considered the DCR equation with constant coefficients. Samec and Škerget [10] in 2004, Rocca et al. [11] in 2005, and AL-Bayati and Wrobel [12,13] in 2018 studied the DCR equation with variable velocity. Martinez et al. [14] in 2013 used nonstandard finite difference schemes based on Green's function formulations for reaction–diffusion–convection systems. Only a limited number of studies on the steady-state equation of variable coefficients have been performed (see, for example, [15]).

This paper is aimed at studying problems that are governed by a DCR equation with variable coefficients. Specifically, this paper will extend the recently published work of [15] on the steady-state DCR equation to the unsteady-state DCR equation of variable coefficients (for anisotropic functionally graded materials) of the form

$$\frac{\partial}{\partial x_i}\left[d_{ij}(\mathbf{x})\frac{\partial c(\mathbf{x},t)}{\partial x_j}\right]-\frac{\partial}{\partial x_i}[v_i(\mathbf{x})c(\mathbf{x},t)]-k(\mathbf{x})c(\mathbf{x},t)=\alpha(\mathbf{x},t)\frac{\partial c(\mathbf{x},t)}{\partial t} \tag{1}$$

The continuously varying coefficients d_{ij}, v_i, k, α in (1) represent the anisotropic diffusivity, velocity, decay reaction, and change rate coefficients of the medium of interest, respectively. Therefore, Equation (1) is relevant for FGMs. Equation (1) covers a wider class of problems since it applies to anisotropic and inhomogeneous media, nonetheless including the case of isotropic diffusion taking place when $d_{11}=d_{22}, d_{12}=0$ as well as the case of homogeneous media that appear when the coefficients $d_{ij}(\mathbf{x})$, $v_i(\mathbf{x})$, $k(\mathbf{x})$ and $\alpha(\mathbf{x},t)$ are constant.

2. The Governing Equation, Initial and Boundary Conditions

Referring to the Cartesian frame Ox_1x_2, we will discuss the initial boundary value problems governed by (1) where $\mathbf{x}=(x_1,x_2)$. The coefficient $\left[d_{ij}\right]$ $(i,j=1,2)$ is a real positive definite symmetrical matrix. Moreover, in (1), the summation convention for repeated indices applies, so (1) can explicitly be written as

$$\begin{aligned}&\frac{\partial}{\partial x_1}\left(d_{11}\frac{\partial c}{\partial x_1}\right)+\frac{\partial}{\partial x_1}\left(d_{12}\frac{\partial c}{\partial x_2}\right)+\frac{\partial}{\partial x_2}\left(d_{12}\frac{\partial c}{\partial x_1}\right)+\frac{\partial}{\partial x_2}\left(d_{22}\frac{\partial c}{\partial x_2}\right)\\&-\frac{\partial}{\partial x_1}(v_1c)-\frac{\partial}{\partial x_2}(v_2c)-kc=\alpha\frac{\partial c}{\partial t}\end{aligned} \tag{2}$$

By knowing the coefficients of $d_{ij}(\mathbf{x}), v_i(\mathbf{x}), k(\mathbf{x}), \alpha(\mathbf{x},t)$, solutions $c(\mathbf{x},t)$ to (1) and its derivatives will be sought within the time interval $t\geq 0$ and region Ω in R^2, with boundary $\partial\Omega$ consisting of a finite number of piecewise smooth curves. On $\partial\Omega_1$, the dependent variable $c(\mathbf{x},t)$ is specified, and

$$F(\mathbf{x},t)=d_{ij}(\mathbf{x})\frac{\partial c(\mathbf{x},t)}{\partial x_i}n_j \tag{3}$$

is specified on $\partial\Omega_2$, where $\partial\Omega=\partial\Omega_1\cup\partial\Omega_2$ and $\mathbf{n}=(n_1,n_2)$ represents the outward pointing normal to $\partial\Omega$. The initial condition is

$$c(\mathbf{x},0)=0 \tag{4}$$

3. Derivation of an Integral Equation

We restrict the coefficients d_{ij}, v_i, k, α to be of the form

$$d_{ij}(\mathbf{x}) = \hat{d}_{ij}\,h(\mathbf{x}) \tag{5}$$
$$v_i(\mathbf{x}) = \hat{v}_i\,h(\mathbf{x}) \tag{6}$$
$$k(\mathbf{x}) = \hat{k}\,h(\mathbf{x}) \tag{7}$$
$$\alpha(\mathbf{x},t) = \hat{\alpha}(t)h(\mathbf{x}) \tag{8}$$

where $h(\mathbf{x})$ is a differentiable function; $\hat{d}_{ij}, \hat{v}_i, \hat{k}$ are constants; and $\hat{\alpha}(t)$ is a function of time t. The substitution of (5)–(8) into (1) gives

$$\hat{d}_{ij}\frac{\partial}{\partial x_i}\left(h\frac{\partial c}{\partial x_j}\right)-\hat{v}_i\frac{\partial(hc)}{\partial x_i}-\hat{k}hc=\hat{\alpha}h\frac{\partial c}{\partial t} \tag{9}$$

Assume

$$c(\mathbf{x},t)=h^{-1/2}(\mathbf{x})\psi(\mathbf{x},t) \tag{10}$$

Therefore, using (5) and (10) in (3) gives

$$F(\mathbf{x},t) = -F_h(\mathbf{x})\psi(\mathbf{x},t) + h^{1/2}(\mathbf{x})F_\psi(\mathbf{x},t) \tag{11}$$

where

$$F_h(\mathbf{x}) = \hat{d}_{ij}\frac{\partial h^{1/2}(\mathbf{x})}{\partial x_j}n_i \qquad F_\psi(\mathbf{x},t) = \hat{d}_{ij}\frac{\partial \psi(\mathbf{x},t)}{\partial x_j}n_i \tag{12}$$

Moreover, Equation (9) can be written as

$$\hat{d}_{ij}\frac{\partial}{\partial x_i}\left[h\frac{\partial\left(h^{-1/2}\psi\right)}{\partial x_j}\right] - \hat{v}_i\frac{\partial\left(h^{1/2}\psi\right)}{\partial x_i} - \hat{k}h^{1/2}\psi = \hat{\alpha}h\frac{\partial\left(h^{-1/2}\psi\right)}{\partial t} \tag{13}$$

That is,

$$\hat{d}_{ij}\frac{\partial}{\partial x_i}\left[h\left(h^{-1/2}\frac{\partial\psi}{\partial x_j} + \psi\frac{\partial h^{-1/2}}{\partial x_j}\right)\right] - \hat{v}_i\left(h^{1/2}\frac{\partial\psi}{\partial x_i} + \psi\frac{\partial h^{1/2}}{\partial x_i}\right) - \hat{k}h^{1/2}\psi = \hat{\alpha}h\left(h^{-1/2}\frac{\partial\psi}{\partial t}\right) \tag{14}$$

or

$$\hat{d}_{ij}\frac{\partial}{\partial x_i}\left(h^{1/2}\frac{\partial\psi}{\partial x_j} + h\psi\frac{\partial h^{-1/2}}{\partial x_j}\right) - \hat{v}_i\left(h^{1/2}\frac{\partial\psi}{\partial x_i} + \psi\frac{\partial h^{1/2}}{\partial x_i}\right) - \hat{k}h^{1/2}\psi = \hat{\alpha}h^{1/2}\frac{\partial\psi}{\partial t} \tag{15}$$

Using the identity

$$\frac{\partial h^{-1/2}}{\partial x_i} = -h^{-1}\frac{\partial h^{1/2}}{\partial x_i} \tag{16}$$

implies

$$\hat{d}_{ij}\frac{\partial}{\partial x_i}\left(h^{1/2}\frac{\partial\psi}{\partial x_j} - \psi\frac{\partial h^{1/2}}{\partial x_j}\right) - \hat{v}_i\left(h^{1/2}\frac{\partial\psi}{\partial x_i} + \psi\frac{\partial h^{1/2}}{\partial x_i}\right) - \hat{k}h^{1/2}\psi = \hat{\alpha}h^{1/2}\frac{\partial\psi}{\partial t} \tag{17}$$

Rearranging and neglecting some zero terms gives

$$h^{1/2}\left(\hat{d}_{ij}\frac{\partial^2\psi}{\partial x_i\partial x_j} - \hat{v}_i\frac{\partial\psi}{\partial x_i}\right) - \psi\left(\hat{d}_{ij}\frac{\partial^2 h^{1/2}}{\partial x_i\partial x_j} + \hat{v}_i\frac{\partial h^{1/2}}{\partial x_i}\right) - \hat{k}h^{1/2}\psi = \hat{\alpha}h^{1/2}\frac{\partial\psi}{\partial t} \tag{18}$$

so that if h satisfies

$$\hat{d}_{ij}\frac{\partial^2 h^{1/2}}{\partial x_i\partial x_j} + \hat{v}_i\frac{\partial h^{1/2}}{\partial x_i} - \lambda h^{1/2} = 0 \tag{19}$$

where λ is a constant, then the transformation (10) takes the variable coefficient Equation (1) into a constant coefficient equation:

$$\hat{d}_{ij}\frac{\partial^2\psi}{\partial x_i\partial x_j} - \hat{v}_i\frac{\partial\psi}{\partial x_i} - \left(\lambda + \hat{k}\right)\psi = \hat{\alpha}\frac{\partial\psi}{\partial t} \tag{20}$$

Taking the Laplace transform of (10), (11), (20) and applying the initial condition (4), we obtain

$$\psi^*(\mathbf{x},s) = h^{1/2}(\mathbf{x})c^*(\mathbf{x},s) \tag{21}$$

$$F_{\psi^*}(\mathbf{x},s) = [F^*(\mathbf{x},s) + F_h(\mathbf{x})\psi^*(\mathbf{x},s)]h^{-1/2}(\mathbf{x}) \tag{22}$$

$$\hat{d}_{ij}\frac{\partial^2\psi^*}{\partial x_i\partial x_j} - \hat{v}_i\frac{\partial\psi^*}{\partial x_i} - \left(\lambda + \hat{k} + s\hat{\alpha}^*\right)\psi^* = 0 \tag{23}$$

Using the Gauss divergence theorem, Equation (23) can be transformed into a boundary integral equation:

$$\begin{aligned}\eta(\boldsymbol{\zeta})\,\psi^*(\boldsymbol{\zeta},s) \quad &= \quad \int_{\partial\Omega}\{F_{\psi^*}(\mathbf{x},s)\,\Phi(\mathbf{x},\boldsymbol{\zeta}) - [F(\mathbf{x})\,\Phi(\mathbf{x},\boldsymbol{\zeta}) \\ &\quad + \Gamma(\mathbf{x},\boldsymbol{\zeta})]\psi^*(\mathbf{x},s)\}dS(\mathbf{x}) \end{aligned} \tag{24}$$

where $\eta = 0$ if $\zeta \notin \Omega$, $\eta = 1/2$ if $\zeta \in \partial\Omega$, $\eta = 1$ if $\zeta \in \Omega$, $F_v(\mathbf{x}) = \hat{v}_i n_i(\mathbf{x})$. For 2D problems, the fundamental solutions $\Phi(\mathbf{x},\boldsymbol{\zeta})$ and $\Gamma(\mathbf{x},\boldsymbol{\zeta})$ are given as

$$\Phi(\mathbf{x},\boldsymbol{\zeta}) \quad = \quad \frac{\rho_i}{2\pi D}\exp\left(-\frac{\dot{\mathbf{v}}.\dot{\mathbf{R}}}{2D}\right)K_0(\mu\dot{R}) \tag{25}$$

$$\Gamma(\mathbf{x},\boldsymbol{\zeta}) \quad = \quad \hat{d}_{ij}\frac{\partial\Phi(\mathbf{x},\boldsymbol{\zeta})}{\partial x_j}n_i \tag{26}$$

where

$$\mu \quad = \quad \sqrt{(\dot{v}/2D)^2 + \left[\left(\lambda + \hat{k} + s\hat{\alpha}^*\right)/D\right]} \tag{27}$$

$$D \quad = \quad \left[\hat{d}_{11} + 2\hat{d}_{12}\rho_r + \hat{d}_{22}\left(\rho_r^2 + \rho_i^2\right)\right]/2 \tag{28}$$

$$\dot{\mathbf{R}} \quad = \quad \dot{\mathbf{x}} - \dot{\boldsymbol{\zeta}} \tag{29}$$

$$\dot{\mathbf{x}} \quad = \quad (x_1 + \rho_r x_2, \rho_i x_2) \tag{30}$$

$$\dot{\boldsymbol{\zeta}} \quad = \quad (\zeta_1 + \rho_r\zeta_2, \rho_i\zeta_2) \tag{31}$$

$$\dot{\mathbf{v}} \quad = \quad (\hat{v}_1 + \rho_r\hat{v}_2, \rho_i\hat{v}_2) \tag{32}$$

$$\dot{R} \quad = \quad \sqrt{(x_1 + \rho_r x_2 - \zeta_1 - \rho_r\zeta_2)^2 + (\rho_i x_2 - \rho_i\zeta_2)^2} \tag{33}$$

$$\dot{v} \quad = \quad \sqrt{(\hat{v}_1 + \rho_r\hat{v}_2)^2 + (\rho_i\hat{v}_2)^2} \tag{34}$$

and ρ_r and ρ_i are the real and the positive imaginary parts of the complex root ρ of the quadratic equation $\hat{d}_{11} + 2\hat{d}_{12}\rho + \hat{d}_{22}\rho^2 = 0$, respectively, and K_0 is the modified Bessel function. Using (21) and (22) in (24) yields

$$\eta h^{1/2}c^* = \int_{\partial\Omega}\left\{\left(h^{-1/2}\Phi\right)F^* + \left[\left(F_h - F_v h^{1/2}\right)\Phi - h^{1/2}\Gamma\right]c^*\right\}dS \tag{35}$$

Equation (35) provides a boundary integral equation for determining the numerical solutions of c^* and its derivatives at all points of Ω. The derivative solutions $\partial c^*/\partial\zeta_1$ and $\partial c^*/\partial\zeta_2$ can be determined using the following equations:

$$\frac{\partial c^*}{\partial\zeta_1} = h^{-1/2}\left[\int_{\partial\Omega}\left\{\left(h^{-1/2}\frac{\partial\Phi}{\partial\zeta_1}\right)F^* + \left[\left(F_h - F_v h^{1/2}\right)\frac{\partial\Phi}{\partial\zeta_1} - h^{1/2}\frac{\partial\Gamma}{\partial\zeta_1}\right]c^*\right\}dS - c^*\frac{\partial h^{1/2}}{\partial\zeta_1}\right] \tag{36}$$

$$\frac{\partial c^*}{\partial\zeta_2} = h^{-1/2}\left[\int_{\partial\Omega}\left\{\left(h^{-1/2}\frac{\partial\Phi}{\partial\zeta_2}\right)F^* + \left[\left(F_h - F_v h^{1/2}\right)\frac{\partial\Phi}{\partial\zeta_2} - h^{1/2}\frac{\partial\Gamma}{\partial\zeta_2}\right]c^*\right\}dS - c^*\frac{\partial h^{1/2}}{\partial\zeta_2}\right] \tag{37}$$

Knowing the solutions of $c^*(\mathbf{x},s)$ and its derivatives $\partial c^*/\partial x_1$ and $\partial c^*/\partial x_2$ from (35), the numerical Laplace transform inversion technique using the Stehfest formula is then employed to find the values of $c(\mathbf{x},t)$ and its derivatives $\partial c/\partial x_1$ and $\partial c/\partial x_2$. The Stehfest formula is

$$
\begin{aligned}
c(\mathbf{x},t) &\simeq \frac{\ln 2}{t}\sum_{m=1}^{N} V_m c^*(\mathbf{x},s_m) \\
\frac{\partial c(\mathbf{x},t)}{\partial x_1} &\simeq \frac{\ln 2}{t}\sum_{m=1}^{N} V_m \frac{\partial c^*(\mathbf{x},s_m)}{\partial x_1} \\
\frac{\partial c(\mathbf{x},t)}{\partial x_2} &\simeq \frac{\ln 2}{t}\sum_{m=1}^{N} V_m \frac{\partial c^*(\mathbf{x},s_m)}{\partial x_2}
\end{aligned} \tag{38}
$$

where

$$
s_m = \frac{\ln 2}{t} m \tag{39}
$$

$$
V_m = (-1)^{\frac{N}{2}+m} \sum_{k=\left[\frac{m+1}{2}\right]}^{\min\left(m,\frac{N}{2}\right)} \frac{k^{N/2}(2k)!}{\left(\frac{N}{2}-k\right)!k!(k-1)!(m-k)!(2k-m)!} \tag{40}
$$

Possible multiparameter solutions $h(\mathbf{x})$ to (19) are

$$
h(\mathbf{x}) = \begin{cases} \text{constant}, \lambda = 0 \\ [\exp(\beta_0 + \beta_i x_i)]^2, \hat{d}_{ij}\beta_i\beta_j + \hat{v}_i\beta_i - \lambda = 0 \end{cases} \tag{41}
$$

If the flow is incompressible, that is, the divergence of the velocity is zero, then

$$
\frac{\partial v_i(\mathbf{x})}{\partial x_i} = 0 \tag{42}
$$

Therefore, the governing Equation (1) reduces to

$$
\frac{\partial}{\partial x_i}\left[d_{ij}(\mathbf{x})\frac{\partial c(\mathbf{x},t)}{\partial x_j}\right] - v_i(\mathbf{x})\frac{\partial c(\mathbf{x},t)}{\partial x_i} - k(\mathbf{x})c(\mathbf{x},t) = \alpha(\mathbf{x})\frac{\partial c(\mathbf{x},t)}{\partial t} \tag{43}
$$

Moreover, from (6), we obtain

$$
\frac{\partial v_i(\mathbf{x})}{\partial x_i} = 2h^{1/2}(\mathbf{x})\hat{v}_i\frac{\partial h^{1/2}(\mathbf{x})}{\partial x_i} = 0 \tag{44}
$$

so that

$$
\hat{v}_i\frac{\partial h^{1/2}(\mathbf{x})}{\partial x_i} = 0 \tag{45}
$$

Therefore, Equation (19) reduces to

$$
\hat{d}_{ij}\frac{\partial^2 h^{1/2}}{\partial x_i \partial x_j} - \lambda h^{1/2} = 0 \tag{46}
$$

Thus, for incompressible flow, possible multiparameter functions $h(\mathbf{x})$ satisfying (46) are

$$
h(\mathbf{x}) = \begin{cases} (\beta_0 + \beta_i x_i)^2, \lambda = 0 \\ [\cos(\beta_0 + \beta_i x_i) + \sin(\beta_0 + \beta_i x_i)]^2, \hat{d}_{ij}\beta_i\beta_j + \lambda = 0 \\ [\exp(\beta_0 + \beta_i x_i)]^2, \hat{d}_{ij}\beta_i\beta_j - \lambda = 0 \end{cases} \tag{47}
$$

4. Numerical Examples

We will examine multiple analytical and nonanalytical test problems to demonstrate the accuracy and effectiveness of the mixed Laplace transform and a boundary element method used in deriving the boundary integral Equation (35). We will also analyze the efficiency, accuracy, and consistency of the combined LT-BEM method.

We assume each problem belongs to a system that is valid in spatial and temporal domains and is governed by Equation (1). The system is also assumed to satisfy the initial condition (4) and some boundary conditions, as mentioned in Section 2. The characteristics of the system, which are represented by the coefficients $d_{ij}(\mathbf{x}), v_i(\mathbf{x}), k(\mathbf{x}), \alpha(\mathbf{x}, t)$ in Equation (1), are assumed to be of forms (5)–(8). They represent, respectively, the diffusivity or conductivity, the velocity of flow existing in the system, the reaction coefficient, and the change rate of the unknown or dependent variable $c(\mathbf{x}, t)$.

A standard BEM with constant elements is employed to obtain numerical results. For simplicity, a unit square depicted in Figures 1 and 2 is taken as the geometrical domain for all problems. A total of 320 elements of equal length, namely 80 elements on each side of the unit square, are used.

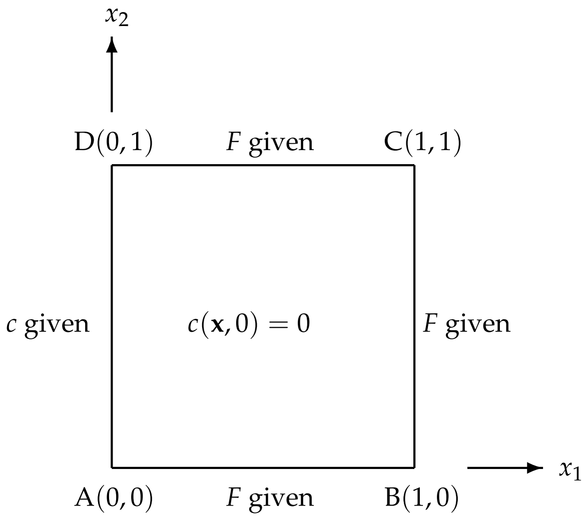

Figure 1. The boundary conditions for problems in Section 4.1.

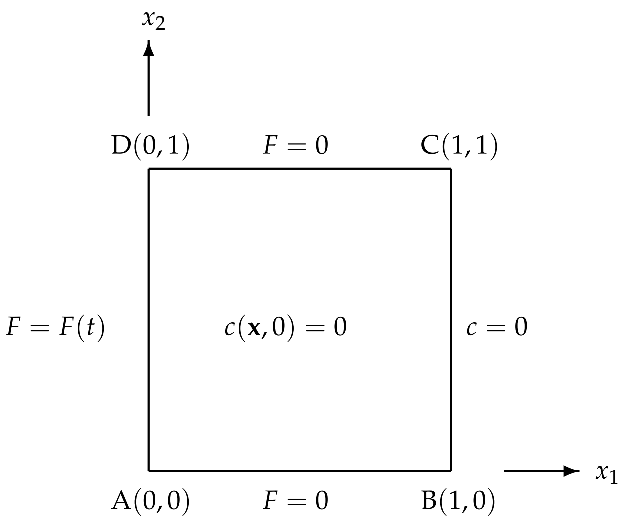

Figure 2. The boundary conditions for problems in Section 4.2.

A FORTRAN script is developed to compute the numerical solutions. A subroutine that evaluates the values of the coefficients $V_m, m = 1, 2, \ldots, N$ of the Stehfest formula in (38) for any number N is embedded in the script. Table 1 shows the values of V_m for $N = 6, 8, 10, 12$ resulting from the subroutine.

Table 1. Values of V_m of the Stehfest formula for $N = 6, 8, 10, 12$.

V_m	$N=6$	$N=8$	$N=10$	$N=12$
V_1	1	−1/3	1/12	−1/60
V_2	−49	145/3	−385/12	961/60
V_3	366	−906	1279	−1247
V_4	−858	16,394/3	−46,871/3	82,663/3
V_5	810	−43,130/3	505,465/6	−1,579,685/6
V_6	−270	18,730	−236,957.5	1,324,138.7
V_7		−35,840/3	1,127,735/3	−58,375,583/15
V_8		8960/3	−1,020,215/3	21,159,859/3
V_9			16,4062.5	−8,005,336.5
V_{10}			−32,812.5	5,552,830.5
V_{11}				−215,5507.2
V_{12}				359,251.2

4.1. A Test Problem

The problems will consider three types of inhomogeneity functions $h(\mathbf{x})$, namely the exponential function of form (41) with the compressible flow, and the quadratic and trigonometric functions of form (47) with incompressible flow. For all test problems, we take coefficients $\hat{d}_{ij}$ and $\hat{k}$

$$\hat{d}_{ij} = \begin{bmatrix} 1 & 0.35 \\ 0.35 & 0.25 \end{bmatrix}, \qquad \hat{k} = 0.5 \tag{48}$$

and a set of boundary conditions (see Figure 1)

F is given on side AB, BC, CD
c is given on side AD

For each problem, numerical solutions of c and its derivatives $\partial c/\partial x_1$and $\partial c/\partial x_2$ are sought at 19×19 interior points $(x_1, x_2) = \{0.05, 0.1, 0.15, \ldots, 0.9, 0.95\} \times \{0.05, 0.1, 0.15, \ldots, 0.9, 0.95\}$ and 9 time-steps $t = 0.0004, \frac{\pi}{8}, \frac{\pi}{4}, \frac{3\pi}{8}, \frac{\pi}{2}, \frac{5\pi}{8}, \frac{3\pi}{4}, \frac{7\pi}{8}, \pi$. The value $t = 0.0004$ is the approximating value of $t = 0$ as the singularity of the Stehfest formula. The individual relative error E_I at each interior point and the aggregate relative error E_A of the numerical solutions are computed using the formulas

$$E_I = \left| \frac{c_{n,i} - c_{a,i}}{c_{a,i}} \right| \tag{49}$$

$$E_A = \left[\frac{\sum_{i=1}^{19\times19} (c_{n,i} - c_{a,i})^2}{\sum_{i=1}^{19\times19} c_{a,i}^2} \right]^{\frac{1}{2}} \tag{50}$$

where c_n and c_a are the numerical and analytical solutions of c or its derivatives, respectively.

Case 1:

First, we suppose that the function $h(\mathbf{x})$ is an exponential function:

$$h(\mathbf{x}) = [\exp(1 + 0.15x_1 - 0.25x_2)]^2 \tag{51}$$

that is, the material under consideration is exponentially graded material. We choose

$$\hat{v}_i = (1,1) \tag{52}$$
$$\hat{\alpha}(t) = 0.192625t \tag{53}$$

so that the system has a compressible flow, as the divergence of the velocity $v_i(x)$ does not equal zero. In order for $h(\mathbf{x})$ to satisfy (41), then $\lambda = -0.088125$. The analytical solution $c(\mathbf{x}, t)$ for this problem is

$$c(\mathbf{x}, t) = \frac{t \exp[-(0.2x_1 + 0.3x_2)]}{\exp(1 + 0.15x_1 - 0.25x_2)}. \tag{54}$$

Figure 3 (top row) shows the aggregate relative errors E_A of the numerical solutions c obtained using $N = 6, 8, 10, 12$ for the Stehfest formula (38). It indicates convergence of the Stehfest formula when the value of N changes from $N = 6$ to $N = 10$. For this specific case (Case 1), the value of N is optimized at $N = 10$. Increasing N to $N = 12$ does not give more accurate solutions. According to Hassanzadeh and Pooladi-Darvish [16], increasing N will increase the accuracy up to a point, and then the accuracy will decline due to round-off errors. The bottom row of Figure 3 depicts individual relative errors E_I for the 19×19 interior points at time $t = \pi/2$ (left) and $t = \pi$ (right), with $N = 10$ as the optimized value of N. It indicates that the errors E_I decrease as t changes from $t = \pi/2$ to $t = \pi$. This result agrees with the result of the aggregate relative error E_A in the top row of Figure 3.

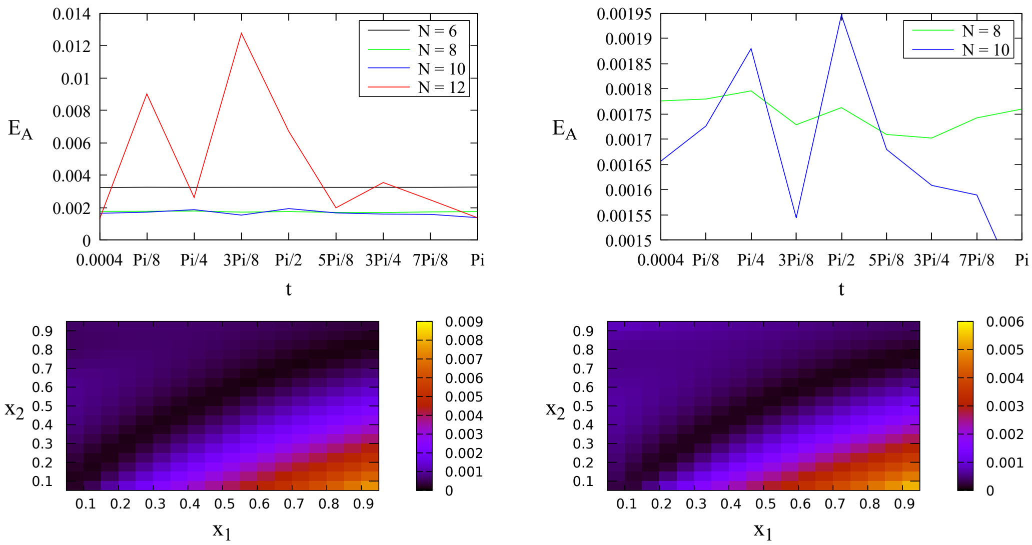

Figure 3. (**Top**): The aggregate relative error E_A of the numerical solutions of c with $N = 6, 8, 10, 12$ for Case 1 (**left**) and zoom-in view for $N = 8, 10$ (**right**). (**Bottom**): The individual relative errors E_I at $t = \pi/2$ (**left**) and $t = \pi$ (**right**) with $N = 10$.

For the derivative solution $\partial c/\partial x_1$, Figure 4 (top row) shows that $N = 6$ is the optimized value of N for the aggregate relative errors E_A. The bottom row of Figure 4 depicts individual relative errors E_I with $N = 6$. It indicates that the errors E_I stay steady as t changes from $t = \pi/2$ to $t = \pi$. This result agrees with the result of the aggregate relative error E_A in the top row of Figure 4.

Meanwhile, for the derivative solution $\partial c/\partial x_2$, Figure 5 (top row) shows that $N = 10$ is the optimized value of N for the aggregate relative errors E_A. The bottom row of Figure 5 depicts individual relative errors E_I with $N = 10$.

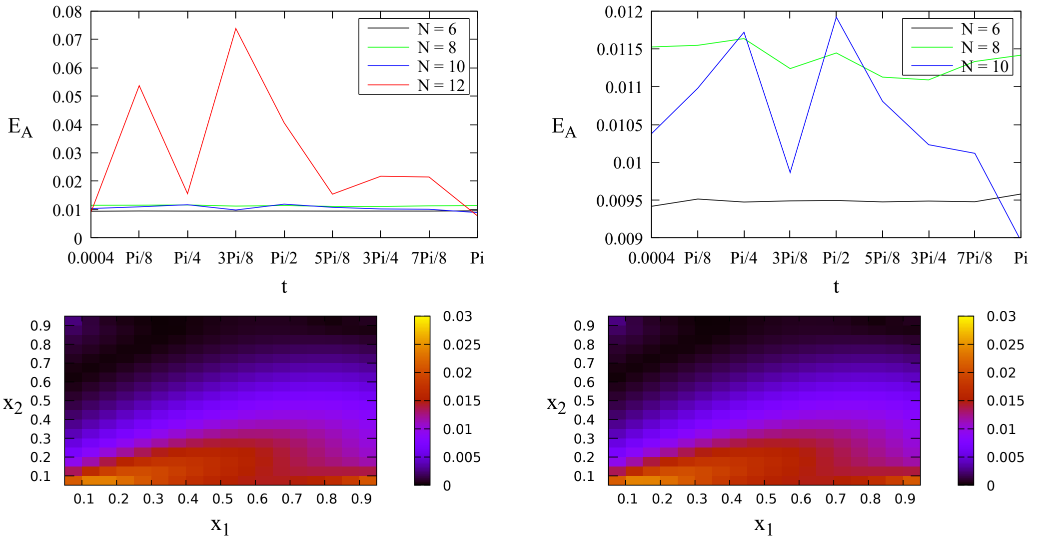

Figure 4. (**Top**): The aggregate relative error E_A of the numerical solutions $\partial c/\partial x_1$ with $N = 6, 8, 10, 12$ for Case 1 (**left**) and zoom-in view for $N = 6, 8, 10$ (**right**). (**Bottom**): The individual relative errors E_I at $t = \pi/2$ (**left**) and $t = \pi$ (**right**) with $N = 6$.

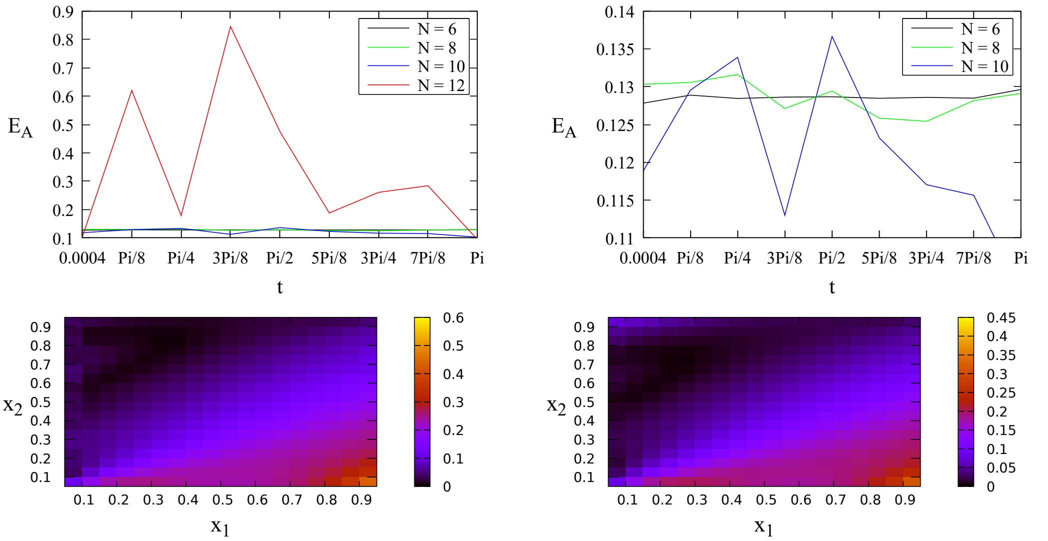

Figure 5. (**Top**): The aggregate relative error E_A of the numerical solutions $\partial c/\partial x_2$ with $N = 6, 8, 10, 12$ for Case 1 (**left**) and zoom-in view for $N = 6, 8, 10$ (**right**). (**Bottom**): The individual relative errors E_I at $t = \pi/2$ (**left**) and $t = \pi$ (**right**) with $N = 10$.

Case 2:

Next, we choose an analytical solution:

$$c(\mathbf{x}, t) = \frac{\exp[-(0.2x_1 + 0.3x_2)]}{1 + 0.15x_1 - 0.25x_2} \sin\sqrt{t} \tag{55}$$

Suppose the function $h(\mathbf{x})$ and the coefficients are

$$h(\mathbf{x}) = (1 + 0.15x_1 - 0.25x_2)^2 \tag{56}$$

$$\hat{v}_i = (1, 0.6) \tag{57}$$

$$\hat{\alpha}(t) = -0.031\sqrt{t}\tan\left(\sqrt{t}\right) \tag{58}$$

Therefore, the considered system involves a quadratically graded material with an incompressible flow. From (47), we have the parameter $\lambda = 0$.

Figure 6 (top row) indicates that $N = 10$ is the optimized value of N for the aggregate relative errors E_A of the numerical solutions of c. Increasing N to $N = 12$ gives worse solutions. The bottom row of Figure 6 depicts individual relative errors E_I with $N = 10$.

$N = 10$ is also the optimized value of N for the aggregate relative errors E_A of the numerical solutions $\partial c/\partial x_1$. This result is shown in Figure 7 (top row). The bottom row of Figure 7 depicts individual relative errors E_I with $N = 10$.

Meanwhile, for the derivative solution $\partial c/\partial x_2$, Figure 8 (top row) shows that $N = 6$ is the optimized value of N for the aggregate relative errors E_A. The bottom row of Figure 8 depicts individual relative errors E_I with $N = 6$.

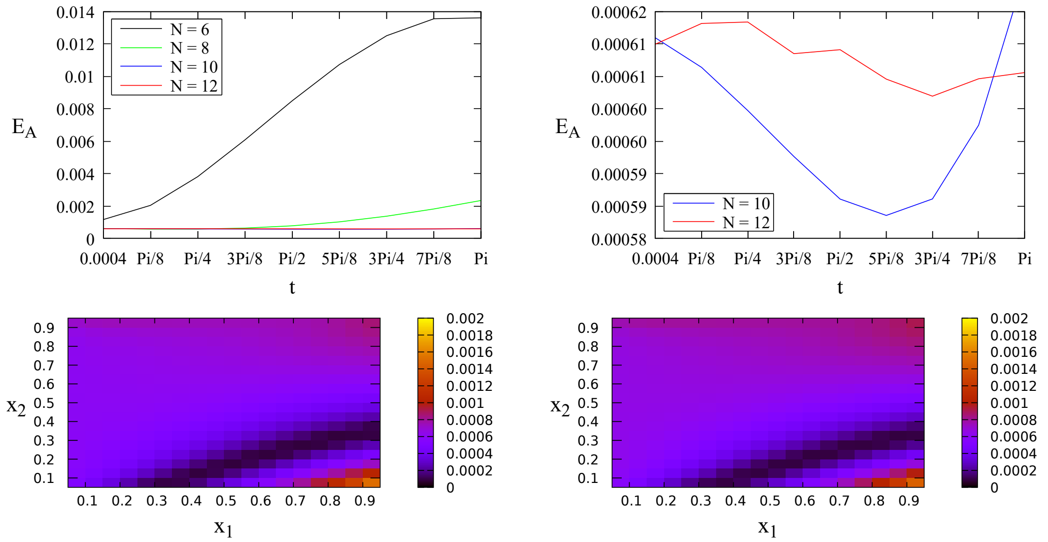

Figure 6. (**Top**): The aggregate relative error E_A of the numerical solutions c with $N = 6, 8, 10, 12$ for Case 2 (**left**) and zoom-in view for $N = 10, 12$ (**right**). (**Bottom**): The individual relative errors E_I at $t = \pi/2$ (**left**) and $t = \pi$ (**right**) with $N = 10$.

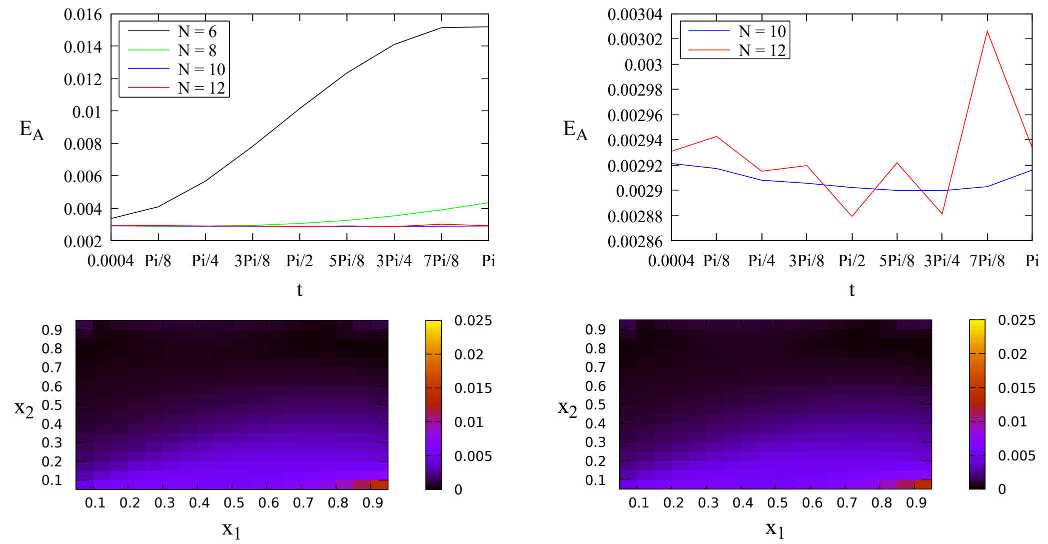

Figure 7. (**Top**): The aggregate relative error E_A of the numerical solutions $\partial c/\partial x_1$ with $N = 6, 8, 10, 12$ for Case 2 (**left**) and zoom-in view for $N = 10, 12$ (**right**). (**Bottom**): The individual relative errors E_I at $t = \pi/2$ (**left**) and $t = \pi$ (**right**) with $N = 10$.

Case 3:

Now, we consider a trigonometrically graded material with a grading function of

$$h(\mathbf{x}) = [\cos(1 + 0.15x_1 - 0.25x_2)]^2 \tag{59}$$

We choose

$$\hat{v}_i = (1, 0.6), \hat{\alpha}(t) = 0.003625[1 - \exp(t)] \tag{60}$$

so that the system has an incompressible flow, as the divergence of the velocity $v_i(x)$ equals zero. From (47) we have $\lambda = -0.011875$. The analytical solution of $c(\mathbf{x}, t)$ for this problem is

$$c(\mathbf{x}, t) = \frac{\exp[-(0.2x_1 + 0.3x_2)][1 - \exp(-t)]}{\cos(1 + 0.15x_1 - 0.25x_2)} \tag{61}$$

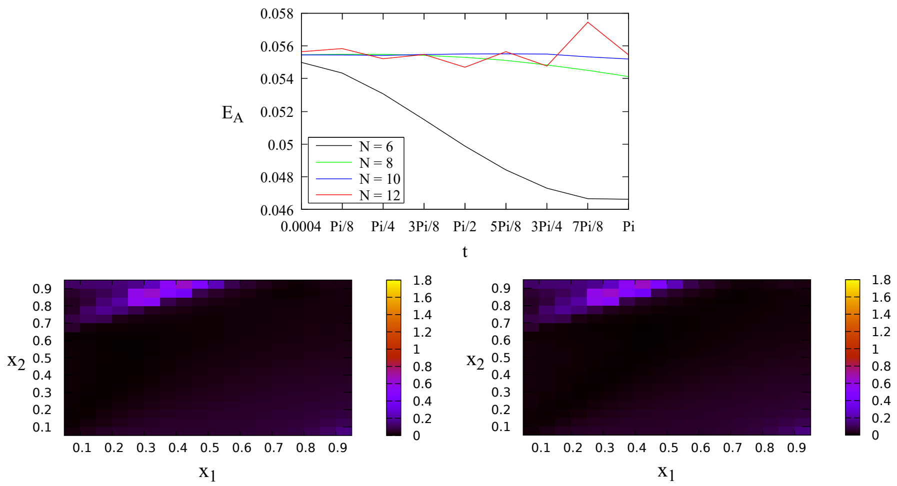

Figure 8. (**Top**): The aggregate relative error E_A of the numerical solutions $\partial c/\partial x_2$ with $N = 6, 8, 10, 12$ for Case 2. (**Bottom**): The individual relative errors E_I at $t = \pi/2$ (**left**) and $t = \pi$ (**right**) with $N = 6$.

Based on the results in Figures 9–11 (top rows) we assume that $N = 12$ is the optimized value for the aggregate relative errors E_A of the solutions of c and the derivatives $\partial c/\partial x_1$ and $\partial c/\partial x_2$. The corresponding individual relative errors E_I are shown in the bottom row of each figure.

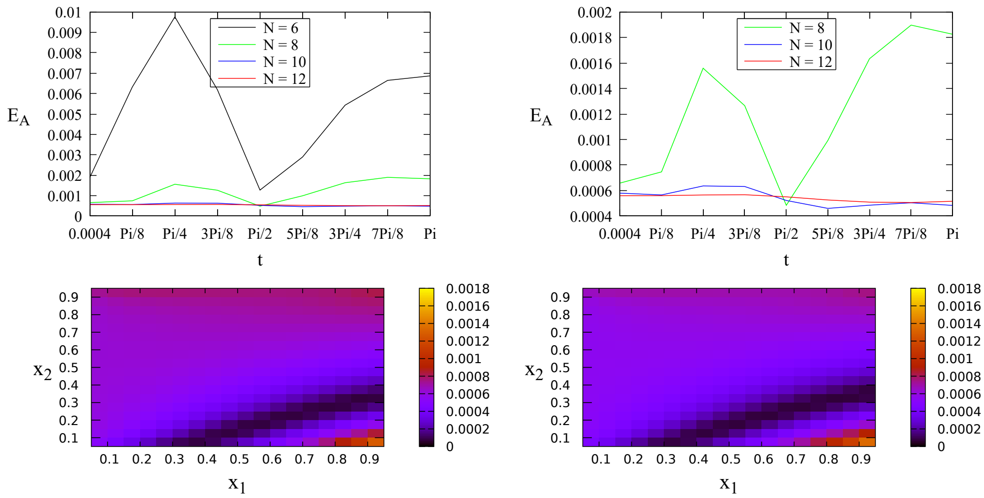

Figure 9. (**Top**): The aggregate relative error E_A of the numerical solutions of c with $N = 6, 8, 10, 12$ for Case 3 (**left**) and zoom-in view for $N = 10, 12$ (**right**). (**Bottom**): The individual relative errors E_I at $t = \pi/2$ (**left**) and $t = \pi$ (**right**) with $N = 12$.

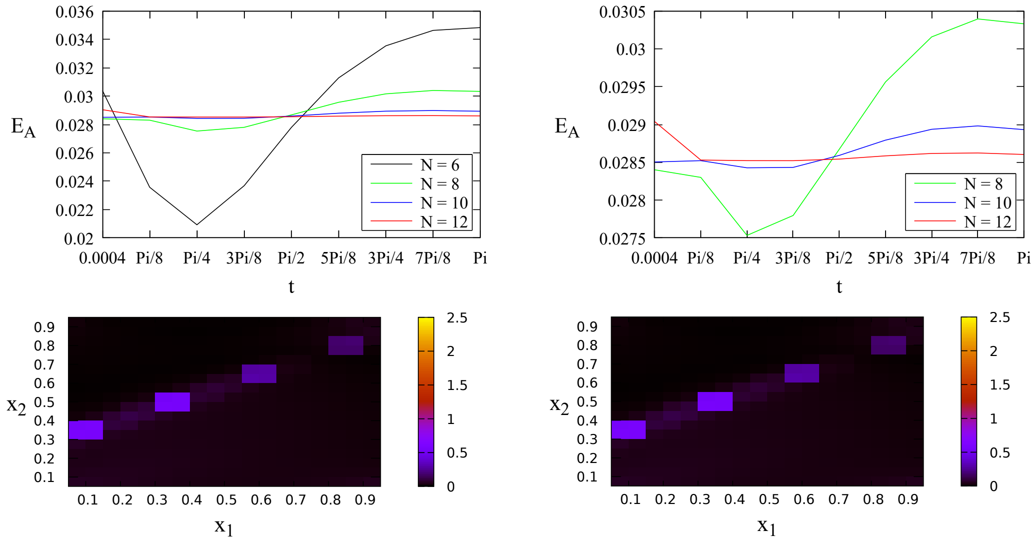

Figure 10. (**Top**): The aggregate relative error E_A of the numerical solutions $\partial c/\partial x_1$ with $N = 6, 8, 10, 12$ for Case 3 (**left**) and zoom-in view for $N = 10, 12$ (**right**). (**Bottom**): The individual relative errors E_I at $t = \pi/2$ (**left**) and $t = \pi$ (**right**) with $N = 12$.

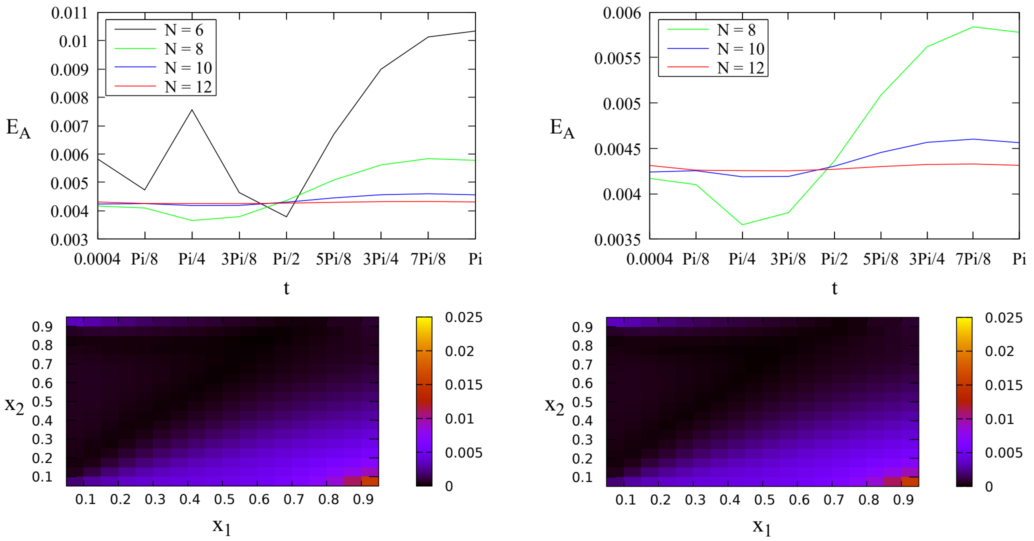

Figure 11. (**Top**): The aggregate relative error E_A of the numerical solutions $\partial c/\partial x_2$ with $N = 6, 8, 10, 12$ for Case 3 (**left**) and zoom-in view for $N = 10, 12$ (**right**). (**Bottom**): The individual relative errors E_I at $t = \pi/2$ (**left**) and $t = \pi$ (**right**) with $N = 12$.

4.2. A Problem without Analytical Solution

Further, we will show that the anisotropy and inhomogeneity of materials give an impact on the solutions. We will use $\hat{d}_{ij}, \hat{v}_i, \hat{k}, h(\mathbf{x})$ in Case 3 of Section 4.1 for this problem, which are

$$\hat{d}_{ij} = \begin{bmatrix} 1 & 0.35 \\ 0.35 & 0.25 \end{bmatrix} \tag{62}$$

$$\hat{v}_i = (1, 0.6) \tag{63}$$

$$\hat{k} = 0.5 \tag{64}$$

$$h(\mathbf{x}) = [\cos(1 + 0.15x_1 - 0.25x_2)]^2 \tag{65}$$

We choose

$$\hat{\alpha}(t) = 1 \tag{66}$$

As we aim to show the impacts of anisotropy and inhomogeneity of the material, we need to consider the case of homogeneous material and the case of isotropic material. We assume that when the material is homogeneous, then

$$h(\mathbf{x}) = 1 \tag{67}$$

and when an isotropic material is under consideration, then

$$\hat{d}_{ij} = \begin{bmatrix} 1 & 0 \\ 0 & 1 \end{bmatrix} \tag{68}$$

The boundary conditions are (see Figure 2)

$$\begin{aligned} &F = 0 \text{ on side AB} \\ &c = 0 \text{ on side BC} \\ &F = 0 \text{ on side CD} \\ &F = F(t) \text{ on side AD} \end{aligned}$$

where $F(t)$ is associated with four cases, namely

$$\begin{aligned} &\text{Case 1:} \quad F(t) = 1 \\ &\text{Case 2:} \quad F(t) = \exp(-t) \\ &\text{Case 3:} \quad F(t) = t \\ &\text{Case 4:} \quad F(t) = t/(t + 0.01) \end{aligned}$$

Figure 12 shows that for all cases, when the material is isotropic and homogeneous, the solutions $c(0.5, 0.3, t)$ and $c(0.5, 0.7, t)$ coincide. This is to be expected, as the problem is geometrically symmetric at $x_2 = 0.5$ when the material is isotropic and homogeneous. Furthermore, the results in Figure 12 also indicate that the material's anisotropy and inhomogeneity affect the solutions. Once we change the material from homogeneous to inhomogeneous, or from isotropic to anisotropic, then the solution will not be symmetric anymore. Moreover, as is also expected, the variation of the solution with respect to t mimics the time function $F(t)$ as the boundary condition on side AD.

Meanwhile, the results in Figure 13 show that Case 1 of $F(t) = 1$ and Case 4 of $F(t) = t/(t + 0.01)$ have the same steady-state solution. This is to be expected, as both the functions $F(t) = 1$ and $F(t) = t/(t + 0.01)$ will converge to 1 when t approaches infinity.

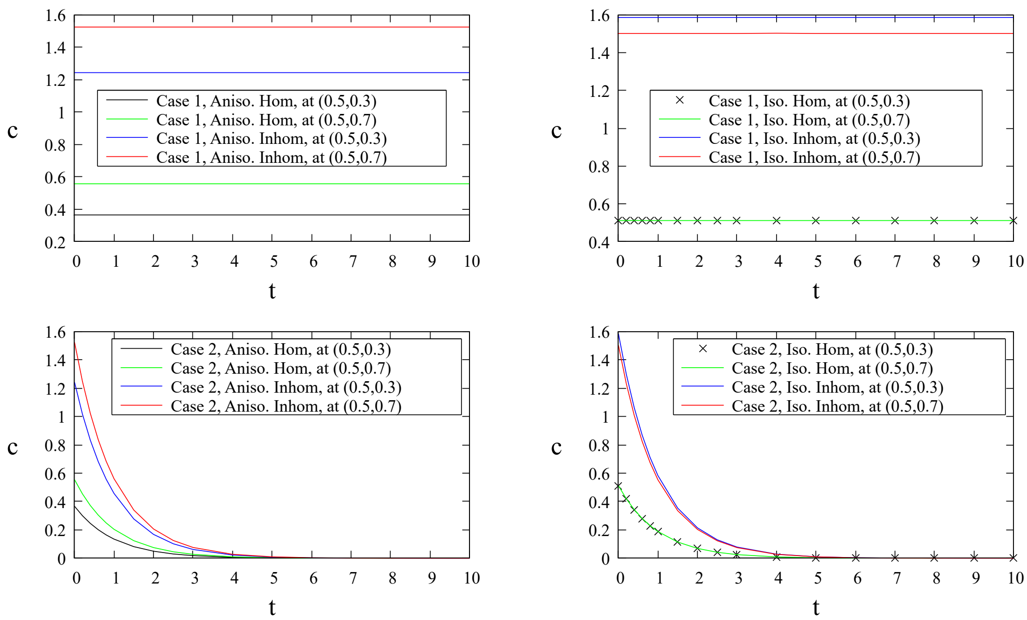

Figure 12. *Cont.*

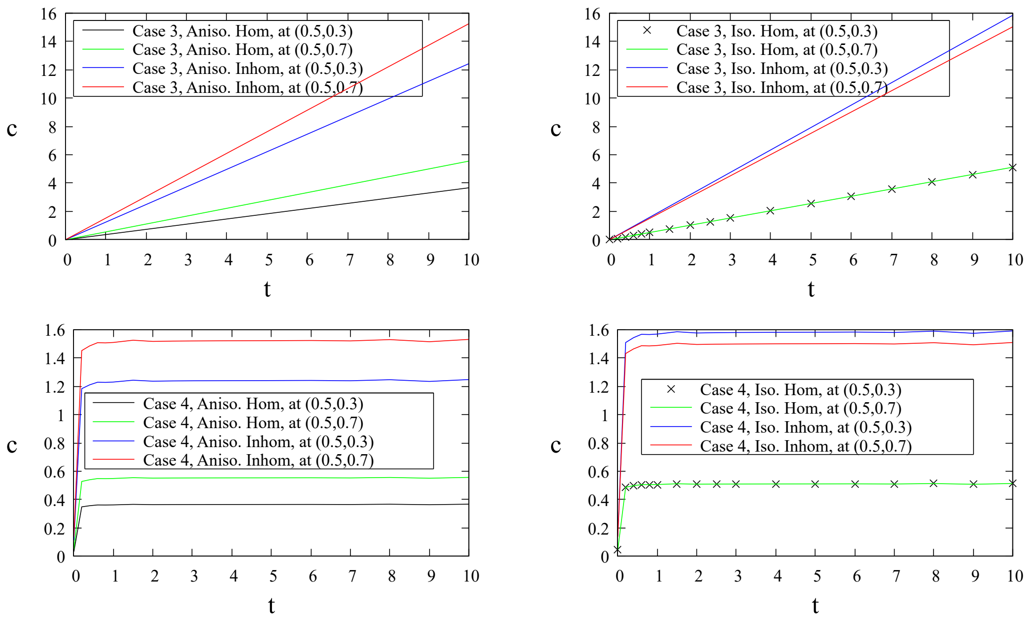

Figure 12. Solutions of $c(0.5, 0.3, t)$ and $c(0.5, 0.7, t)$ for all cases.

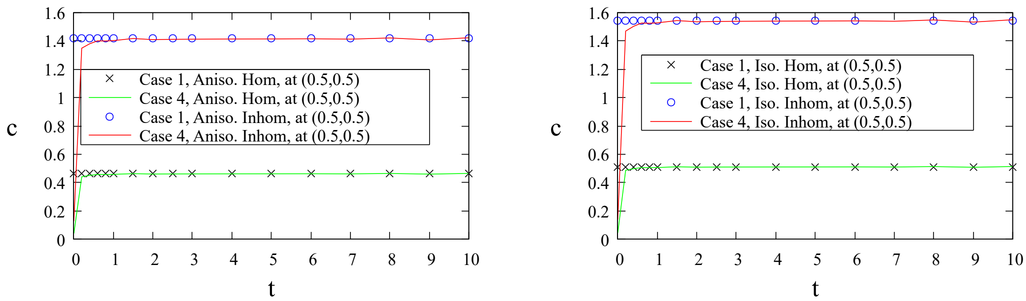

Figure 13. Solutions of $c(0.5, 0.5, t)$ for Case 1 and 4.

5. Conclusions

Two-dimensional transient problems for anisotropic FGMs governed by a diffusion–convection–reaction equation of variable coefficients of the form (1) have been considered. The coefficients $d_{ij}(\mathbf{x}), v_i(\mathbf{x}), k(\mathbf{x}), \alpha(\mathbf{x}, t)$ are restricted to take forms (5), (6), (7) and (8), respectively. By assuming that the gradation function $h(\mathbf{x})$ satisfies (19), and by using the transformation (10), the variable coefficient Equation (1) is reduced to a constant coefficient Equation (20), which can be written in the form of the boundary-only integral Equation (35) and solved using a standard BEM for the solutions c^*. These BEM solutions are then numerically inverse transformed using the Stehfest formula (38) to obtain the solutions c.

Some problems of three types of gradation function $h(\mathbf{x})$, namely trigonometric, exponential, and quadratic functions, have been solved. Based on the results obtained, we may conclude that the analysis of the reduction to the constant coefficient equation (in Section 3) for deriving the boundary-only integral Equation (35) is valid, and the combined BEM and Stehfest formula is quite accurate.

Funding: The APC was funded by Hasanuddin University, Makassar, Indonesia.

Data Availability Statement: The data that support the findings of this study are available within the article.

Acknowledgments: This work is supported by Hasanuddin University and Ministry of Education, Culture, Research, and Technology of Indonesia. The author would like to thank the reviewers for their beneficial comments and suggestions that have improved the paper.

Conflicts of Interest: The author declares no conflict of interest.

Abbreviations

The following abbreviations are used in this manuscript:

FGM	Functionally Graded Material
BEM	Boundary Element Method
LT	Laplace Transform
DCR	Diffusion Convection Reaction

List of Symbols

The following symbols are used in this manuscript:

c	concentration
$\mathbf{x}$	spatial variable
t	temporal variable
d_{ij}	diffusivity
v_i	velocity
k	reaction coefficient
α	rate of change of the concentration
$\partial/\partial x_i, \partial/\partial t$	partial derivative with respect to x_i and t, respectively
$\Omega, \partial\Omega$	the spatial domain and its boundary, respectively
F	flux
h	gradation function
$\hat{d}_{ij}$	constant diffusivity
$\hat{v}_i$	constant velocity
$\hat{k}$	constant reaction coefficient
$\hat{\alpha}$	constant rate of change of the concentration
ψ	transformation function
λ	constant parameter
$*$	the Laplace transform of a dependent variable
s	variable of the Laplace transform
Φ, Γ	the fundamental solutions
ζ	variable of the fundamental solutions
ρ, μ, D	parameters of the fundamental solutions
$\dot{\mathbf{x}}, \dot{\boldsymbol{\zeta}}, \dot{\mathbf{R}}, \dot{\mathbf{v}}$	vectors for the fundamental solutions
$\dot{R}, \dot{v}$	length of the vectors $\dot{\mathbf{R}}, \dot{\mathbf{v}}$, respectively
N, V_m	parameters of the Stehfest formula

References

1. Bear, J. *Dynamics of Fluids in Porous Media*; American Elsevier Publishing Company, Inc.: New York, NY, USA, 1972.
2. Fredlund, D.G.; Rahardjo, H. *Soil Mechanics for Unsaturated Soils*; John Wiley & Sons: Hoboken, NY, USA, 1993.
3. Charbeneau, R.J.; Sherif, S.A. Groundwater Hydraulics and Pollutant Transport. *Appl. Mech. Rev.* **2002**, *55*, B38–B39. [CrossRef]
4. Yan, G.; Li, Z.; Galindo Torres, S.A.; Scheuermann, A.; Li, L. Transient Two-Phase Flow in Porous Media: A Literature Review and Engineering Application in Geotechnics. *Geotechnics* **2022**, *2*, 32–90. [CrossRef]
5. Fendoglu, H.; Bozkaya, C.; Tezer-Sezgin, M. DBEM and DRBEM solutions to 2D transient convection-diffusion-reaction type equations. *Eng. Anal. Bound. Elem.* **2018**, *93*, 124–134. [CrossRef]
6. Wang, X.; Ang, W.-T. A complex variable boundary element method for solving a steady-state advection–diffusion–reaction equation. *Appl. Math. Comput.* **2018**, *321*, 731–744. [CrossRef]
7. Sheu, T.W.H.; Wang, S.K.; Lin, R.K. An Implicit Scheme for Solving the Convection–Diffusion–Reaction Equation in Two Dimensions. *J. Comput. Phys.* **2000**, *164*, 123–142. [CrossRef]
8. Xu, M. A modified finite volume method for convection-diffusion-reaction problems. *Int. J. Heat Mass Transf.* **2018**, *117*, 658–668. [CrossRef]
9. AL-Bayati, S.A.; Wrobel, L.C. Radial integration boundary element method for two-dimensional non-homogeneous convection–diffusion–reaction problems with variable source term. *Eng. Anal. Bound. Elem.* **2019**, *101*, 89–101. [CrossRef]
10. Samec, N.; Škerget, L. Integral formulation of a diffusive–convective transport equation for reacting flows. *Eng. Anal. Bound. Elem.* **2004**, *28*, 1055–1060. [CrossRef]

11. Rocca, A.L.; Rosales, A.H.; Power, H. Radial basis function Hermite collocation approach for the solution of time dependent convection–diffusion problems. *Eng. Anal. Bound. Elem.* **2005**, *29*, 359–370. [CrossRef]
12. AL-Bayati, S.A.; Wrobel, L.C. The dual reciprocity boundary element formulation for convection-diffusion-reaction problems with variable velocity field using different radial basis functions. *Int. J. Mech. Sci.* **2018**, *145*, 367–377. [CrossRef]
13. AL-Bayati, S.A.; Wrobel, L.C. A novel dual reciprocity boundary element formulation for two-dimensional transient convection–diffusion–reaction problems with variable velocity. *Eng. Anal. Bound. Elem.* **2018**, *94*, 60–68. [CrossRef]
14. Hernandez-Martinez, E.; Puebla, H.; Valdes-Parada, F.; Alvarez-Ramirez, J. Nonstandard finite difference schemes based on Green's function formulations for reaction–diffusion–convection systems. *Chem. Eng. Sci.* **2013**, *94*, 245–255. [CrossRef]
15. Azis, M.I. Standard-BEM solutions to two types of anisotropic-diffusion convection reaction equations with variable coefficients. *Eng. Anal. Bound. Elem.* **2019**, *105*, 87–93. [CrossRef]
16. Hassanzadeh, H.; Pooladi-Darvish, M. Comparison of different numerical Laplace inversion methods for engineering applications. *Appl. Math. Comput.* **2007**, *189*, 1966–1981. [CrossRef]